PSFC/JA-23-117

Self-Protection Characteristic Comparison Between No-Insulation, Metal-as-Insulation, and Surface-Shunted-Metal-as-Insulation REBCO Coils

Junseong Kim, Dongkeun Park, Fangliang Dong, Andrew Lanzrath, Wooseung Lee,
Juan Bascuñán, Yukikazu Iwasa

May 2023

Plasma Science and Fusion Center
Massachusetts Institute of Technology
Cambridge MA 02139 USA

This work was supported by the National Institute of General Medical Sciences of the National Institutes of Health under Grant R01GM137138.

Submitted to *IEEE Transactions on Applied Superconductivity*

Self-Protection Characteristic Comparison between No-Insulation, Metal-as-Insulation, and Surface-Shunted-Metal-as-Insulation REBCO coils

Junseong Kim, Dongkeun Park, Fangliang Dong, Andrew Lanzrath, Wooseung Lee, Juan Bascuñán, and Yukikazu Iwasa

***Abstract*— A metal tape co-winding or a metal-as-insulation (MI) winding method is an excellent way to improve the mechanical property and lower the average current density, i.e. lower the stress, of a high-field REBCO magnet without completely losing the benefits of the no-insulation (NI) winding method. However, MI winding will increase the resistance between turns, called the characteristic resistance. The increased characteristic resistance will reduce the bypass current at a quench situation, which may not be desirable from a quench protection point of view. Making a shunt on top of the winding surface of the coil may be a possible solution to control the characteristic resistance. In this presentation, we compare the characteristic resistances and their correlated self-protecting characteristics between NI, MI, and surface-shunted-metal-as-insulation (SSMI). We present the test results of single pancake (SP) coils wound with applying the same winding pressure with the different winding methods, NI, MI, and SSMI. Especially for the SSMI method, we investigate how the method of the surface-shunt affects the characteristic resistance. Based on the results, the authors hope to find a way to control the characteristic resistance value with much more flexibility compared to the simple MI.**

***Index Terms*—Metal-as-insulation, No-insulation, REBCO magnet, Self-protection, Surface-shunted.**

I. Introduction

THE impressive self-protection characteristic of the no-insulation (NI) high-temperature superconducting (HTS) coils has been validated by many experiments. The key idea of the NI winding technique is to completely eliminate turn-to-turn insulation within the HTS winding [1] . When a local hot spot occurs or an external power supply is shut in an NI HTS coil, the current that originally flows in the azimuthal direction through superconducting layer is automatically bypassed to the resistive turn-to-turn path [2]–[4]. This current bypass allows that the coil can flow the current beyond the critical current, I_C, and prevents the coil from overheating and consequently from burning—self-protection. For the conventional insulated HTS magnet, the operating current density cannot be high due to protection issue; generally the maximum allowable matrix current density determines the operating current [5]. With its self-protection characteristic, the NI HTS, here REBCO, magnet can be operated at much higher overall current density (even ≥1500 A/mm^2 [6]) that allows to be much more compact than the conventional insulated magnet. As the recent REBCO conductor's I_C performance at low temperature under high field has improved considerably [7]–[9], high-field magnets can be designed with higher operating current densities and consequently use less conductor length; this is highly desirable as the REBCO conductor is still very expensive.

However, the NI REBCO magnet also encounters the mechanical stress issue as the operating current density increases although it is more robust than the conventional insulated magnet containing more portion of soft materials (insulation, copper). The hoop stress increases in proportion to the current density. If we intend to design high-field magnet having a medium-to-large bore using a high-I_C-performance REBCO conductor, we may have to increase the conductor thickness to adjust the overall current density, and high-strength metal tape co-winding, or called metal-as-insulation (MI), would be better option than use of thicker-copper-plated REBCO tape because of the higher mechanical strength in the winding pack [10], [11]. As this high-strength metal tape such as stainless steel (SS) and Hastelloy has very low electrical conductivity and poor contact resistivity to the adjacent copper layer of REBCO conductor, the turn-to-turn resistance, or characteristic resistance, R_C, can be much greater than the one in the NI winding. That is, the MI coil intrinsically has less self-protecting capability against overheating, overcurrent, and sudden-discharging than the NI coil. In the case of sudden-discharging fault mode, even NI coils can quench in some harsh operating conditions initiated by turn-to-turn heating after the external power supply is shut, and we suggested a quench preventive approach by applying an external shunt resistor across the NI coil. It is obvious that The MI coil is much more vulnerable to quench in this situation. The MI coil seems to be a trade-off method between self-protecting ability and mechanical stress.

We have previously proposed and demonstrated an extra-shunting on NI coils for further enhancement of the self-protecting capability [12]–[14]. In this paper, we expand our

Research reported in this publication was supported by the National Institute of General Medical Sciences of the National Institutes of Health under award number R01GM137138. *(Corresponding author: Dongkeun Park.)*

J. Kim, D. Park, F. Dong, A. Lanzrath, J. Bascuñán, and Y. Iwasa are with the Plasma Science and Fusion Center (PSFC), Massachusetts Institute of Technology (MIT), Cambridge, MA 02139, USA. (e-mail: dk_park@mit.edu).

W. Lee was with the PSFC, MIT, Cambridge, MA 02139, USA. He is now with Gwangju Center, Korea Basic Science Institute, Buk-gu, Gwangju, 611856, South Korea. (e-mail: wlee2022@kbsi.re.kr).

previous experience to the MI winding and present a surface-shunted-metal-as-insulation (SSMI) winding method to secure both mechanical strength and self-protecting capability while keeping decent overall current density within the winding pack. To demonstrate and compare the self-protecting performance, we built and tested three small-scale single-pancake REBCO test coils with NI, MI, and SSMI winding methods.

II. Three Types of Test Coils: NI, MI, and SSMI

We select REBCO tapes with 6-mm width and 76-μm thickness (~10 μm copper on each side) by SuperPower left over from our previous experiment [15] to build three single pancake test coils. The NI coil was wound to 130 turns with a 20-N winding tension on a copper bobbin of a 22.4 mm inner diameter (ID) as shown in Fig. 1a. This copper bobbin is also used a current terminal of this single pancake coil. The outer diameter (OD) of the NI coil is a 42.1 mm. For the MI coil, we used a full-hard SS 304 tape for co-winding. The winding tension of same 20 N were applied to both the REBCO and SS tapes. We intend to make the same 130-turn coils for the MI and the SSMI test coils. Figure 1b shows that the MI coil OD is larger than the NI coil OD because of co-winding, i.e., larger cross-sectional area for the same ampere-turns. As we made the SSMI coil by using the MI coil, coil parameters of the SSMI coil are basically same as the MI coil. Table I shows the parameters and computed inductance of the three coils.

The SSMI coil was made by soldering on the top surface of the early made and test-completed MI coil as shown in Fig. 1c. There have been some preliminary studies on a soldered-metal-insulation coil [17]–[19], but these approaches used pre-tinned tapes and thus thickness of solder layers between turns cannot be negligible, i.e., not targeting to keep a mechanical strength of the MI coil. After completing the test, the MI coil was warmed and dried. The coil was placed on the heat plate and heated up to 80°C to solder by using Cerrolow 136 ($Bi_{49}Pb_{18}In_{21}Sn_{12}$) [16]. To create a surface-shunt after completion of the coil winding that uses an $In_{52}Sn_{48}$ solder (melting point: 118°C) for affixing the end turns on the coil, the lower-temperature solder (or fusible alloy) Cerrolow 136 (melting point: 58°C) was used for soldering not to melt and fail the coil winding during this surface-shunting process. We may use a cold-pressed indium sheets or use different combination of solders in the coil winding and the surface shunt. Table II shows properties of selected solders [16]. Note that the Cerrolow 136 is superconducting at <3 T and below 6.4 K. When we use this solder as a shunt and test at 4.2 K, we may not be able to ramp up the coil because of superconducting shunt – necessary to initially ramp at 10 K.

The three coils were tested at 77 K in a liquid nitrogen bath. We used a Toshiba THS118 (GaAs type) hall sensor and placed at the center of the coils to measure the center field. The power supply current and a voltage across the coil end turns were also measured. For comparing the self-protecting characteristics, we obtained the characteristic resistance, R_C, of the NI, MI, and SSMI by conducting charging and discharging experiments. We also performed over-I_C-current charging tests to compare the thermal runaway characteristic in the liquid-nitrogen cooling condition.

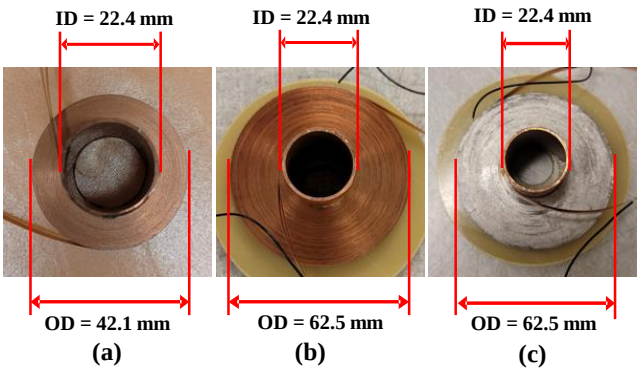

Fig. 1. Photos of three types of NI REBCO test coils: (a) conventional NI; (b) MI; and (c) SSMI coils.

TABLE I
Specification of REBCO Test Coils

Parameter	NI coil	MI coil	SSMI coil
REBCO width; thickness		6 mm; 76 μm	
SS tape width; thickness	N/A	6 mm; 78 μm	
Winding ID; OD [mm]	22.4; 42.1	22.4; 62.5	22.4; 62.5
Number of turns		130	
Total length [m]	13.2	17.4	17.4
Computed inductance [μH]	560	650	650

TABLE II
Properties of Solders

Solder	Melting Point [°C]	ρ (300K) [10^{-7}Ω·m]	ρ (77K) [10^{-7}Ω·m]	T_C [K]	B_{C2} [T]
Cerrolow 136	58	9.4	8.1	6.4	3.3
$In_{52}Sn_{48}$	118	2.6	1.3	6.4	0.34
$Pb_{38}Sn_{62}$	183	1.5	0.48	7.3	0.3

III. Results and Discussion

First, we measured the critical current, I_C, of each coil at 77K as shown in Fig. 2a. Here, the I_C of the coil was determined based on 0.1 μV/cm for a total length in the winding, i.e., 0.13 mV for NI and 0.17 mV for MI and SSMI coils, and the ramp rate was set to 0.5 A/s. The I_C of the NI coil is lower as 51 A than the other coils (MI=79 A, SSMI=81 A) because of the overall current density is higher and thus the field in the coil is higher. A difference in I_C between the MI and SSMI, basically the same coil except surface shunted, comes from a different turn-to-turn resistance which affects the resistive voltage rise during superconducting to normal transition; a lowered turn-to-turn resistive voltage by the surface shunt in the SSMI results in higher coil I_C in definition here.

The turn-to-turn characteristic resistance, R_C, and turn-to-turn contact resistivity, ρ_C, is widely used as an index to compare the self-protecting performance of NI coils. To obtain these values, the time constant of the coil is required. Next, we conducted a discharging test at the operating current of 20 A

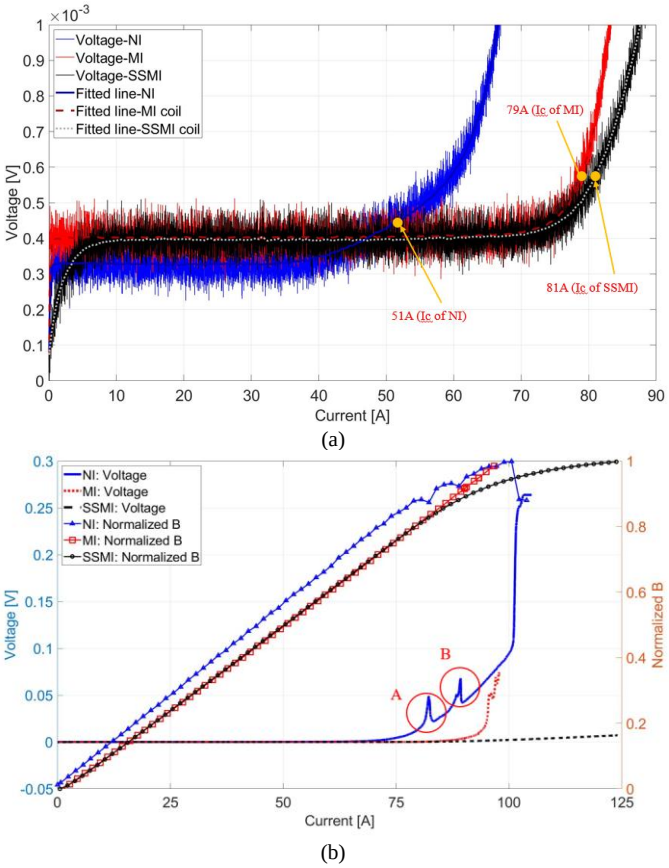

Fig. 2. Experimental results graph for (a) Ic test and (b) over current test.

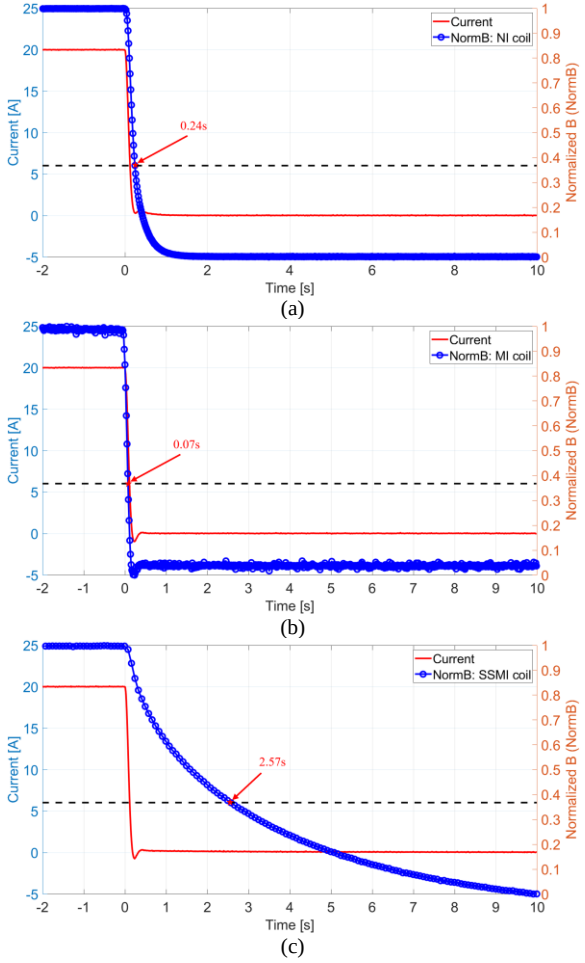

Fig. 3. Results of discharging test of (a) NI, (b) MI, and (c) SSMI HTS coil.

sufficiently lower than I_Cs of each coil by turning off the power supply. The experimental results are represented as graph in Fig. 3. The time constant of each coil obtained through the experiment and is summarized in Table III. By substituting the time constant into (1), the characteristic resistance, R_c, can be obtained.

$$R_c = \frac{L_{coil}}{\tau} \tag{1}$$

Where L_{coil} is the inductance of the coil. The inductance was obtained from the $L_{coil}\cdot dI/dt$ in the current charging sequence and these values are well consistent with the computation in Table I. For removing the influence of the coil shape, the contact surface resistivity, ρ_{ct}, was calculated using (2) because the shape of the NI coil and the MI/SSMI coil are different.

$$R_c = \sum_{i=1}^{N-1} \frac{\rho_{ct}}{2\pi r_i w} \tag{2}$$

Where r_i is the winding radius of the i-th HTS tape, and w is the HTS width. ρ_{ct} was obtained by summing the reciprocal of the length of each turn and then multiplying the obtained R_c. The obtained values are summarized in Table III.

In Fig. 3b, it can be seen that the magnetic field and current of the MI coil are similarly decreased, i.e., the field decay by the power supply not by the time constant of the MI coil. The real time constant must be much higher than obtained time constant by this experiment. Regardless of this difference, the

TABLE III
SPECIFICATION OF COILS

Parameter	NI coil	MI coil	SSMI coil
Inductance [μH]	509.4	651.3	643.5
Critical current, Ic [A]	51	79	81
Time constant, τ [s]	0.24	0.07	2.57
Characteristic resistance, R_c[mΩ]	2.333	9.286	0.2529
Surface contact resistivity, ρ_{ct}[μΩ·cm^2]	105.4	523.9	14.27

ρ_{ct} value of the MI coil is 523.9 μΩ·cm^2 which is sufficiently high compared with the that of the SSMI coil, 14.27 μΩ·cm^2.

Finally, we pushed the power supply current over the I_C of the coils. The results of the over-current charging experiments are shown in Fig. 2b. Figure 2b shows both coil voltages and center fields versus current up to maximum 125 A. Due to higher center field of the NI than other two coils and inaccurate positions of the hall sensor causing field difference, we normalize the field to make a more intuitive comparison. All three coils were charged normally with some delays up to their I_C. For the NI coil, when the current passes its I_C of 51 A, the voltage starts increasing as in Fig. 2a and very slowly increases up to ~67 A. After passing 67 A, the voltage increases more

quickly and after showing two upticks at around 82 A and 89 A, the Point A and B in Fig. 2b, respectively, the NI coil eventually experiences a thermal run-away from the point of passing 100 A; ~50 A above the I_C. We think that the NI coil was partially quenched at Point A (>30 A above the I_C) and it was recovered by the self-protection and the excellent cooling capacity of liquid nitrogen. The partial quench and recovery occurred again at Point B. In the case of the MI coil (Fig. 2b), the voltage increases quite slowly up to ~86 A and then, it gradually increases fast. At around 92 A (13 A above its I_C), the voltage rises rapidly and seems to recover for a while but it rises sharply again—a thermal runaway. Then, we stopped the testing to protect the MI coil to be used for the SSMI too. The first quench point above the I_C, ΔI=13 A, of the MI coil is quite lower than that of the NI coil, ΔI=30 A, and more obviously the NI coil was recovered and eventually quenched at the current point above I_C, ΔI=50 A whereas the MI coil was not recovered and seemed to quench, i.e., the poorer self-protecting capability.

On the other hand, the voltage of the SSMI coil increases very slowly up to 125A (maximum current of our power supply used in this study) which is about 44 A higher than its I_C, more stable than the NI coil. The SSMI did not experience any thermal runaway that means it generates a less turn-to-turn heating during over-I_C current operation than the NI and the MI coils in the same liquid nitrogen cooing condition. We can also find the significant difference in the magnetic field plots between the MI and the SSMI from the point of passing around 86 A. The magnetic field of the SSMI coil was saturated, i.e. the remarkable current was bypassed to the turn-to-turn radial path, here a majority portion of turn-to-turn leak currents through the surface shunt (solder).

Consequently, we demonstrated that the SSMI winding method based on its low turn-to-turn resistance thanks to the surface shunting shows a superior self-protecting capability.

IV. Conclusion

In this paper, we present a promising SS-tape-co-winding NI (or MI) variant, SSMI winding method: 1) to keep the mechanical advantage of MI that can lower the overall-current density, not sacrificing operating current over I_C, and increase the equivalent strength within the winding pack; 2) to enhance the self-protecting capability even better than that of the NI coil. We have demonstrated by comparing three test coils, NI, MI, and SSMI, by conducting over-current and discharging tests that the SSMI coil is thermally stable even in the over-I_C-current region and self-protecting due to its reduced (lowest among three coils) R_C. In addition, since the SSMI winding method requires additional shunting by either soldering or any affixed conductive materials on the already-wound coil surface, the self-protecting capability can be reinforced and ideally controlled by shunting methods after manufacturing and preliminary testing the magnet coils, i.e., a flexible self-protection enhancing method. In order to design and control the turn-to-turn R_C, further studies of the extra-shunted NI/MI winding method by settling a reliable process and by applying different types of metals/solders will be performed in future.

References

[1] S. Hahn, D. K. Park, J. Bascuñán, and Y. Iwasa, "HTS pancake coils without turn-to-turn insulation," *IEEE Trans. Appl. Supercond.*, vol. 21, no. 3 PART 2, pp. 1592–1595, 2011.

[2] X. Wang *et al.*, "Turn-to-turn contact characteristics for an equivalent circuit model of no-insulation ReBCO pancake coil," *Supercond. Sci. Technol.*, vol. 26, no. 3, p. 035012, 2013.

[3] Y. Wang, W. K. Chan, and J. Schwartz, "Self-protection mechanisms in no-insulation (RE)Ba 2 Cu 3 O x high temperature superconductor pancake coils," *Supercond. Sci. Technol.*, vol. 29, no. 4, p. 045007, Apr. 2016.

[4] R. Gyuráki, T. Benkel, F. Schreiner, F. Sirois, and F. Grilli, "Fluorescent thermal imaging of a non-insulated pancake coil wound from high temperature superconductor tape," *Supercond. Sci. Technol.*, vol. 32, no. 10, p. 105006, Oct. 2019.

[5] Y. Iwasa, *Case Studies in Superconducting Magnet*, 2nd ed. Springer, 2009.

[6] Seungyong Hahn, Dong Keun Park, J. Voccio, J. Bascunan, and Y. Iwasa, "No-Insulation (NI) HTS Inserts for $>$1 GHz LTS/HTS NMR Magnets," *IEEE Trans. Appl. Supercond.*, vol. 22, no. 3, pp. 4302405–4302405, Jun. 2012.

[7] A. Molodyk *et al.*, "Development and large volume production of extremely high current density YBa2Cu3O7 superconducting wires for fusion," *Sci. Rep.*, vol. 11, no. 1, p. 2084, Dec. 2021.

[8] M. Paidpilli and V. Selvamanickam, "Development of RE-Ba-Cu-O superconductors in the U.S. for ultra-high field magnets," *Supercond. Sci. Technol.*, vol. 35, no. 4, p. 043001, Apr. 2022.

[9] Honghai Song, P. Brownsey, Yifei Zhang, J. Waterman, T. Fukushima, and D. Hazelton, "2G HTS Coil Technology Development at SuperPower," *IEEE Trans. Appl. Supercond.*, vol. 23, no. 3, pp. 4600806–4600806, Jun. 2013.

[10] T. Lecrevisse and Y. Iwasa, "A (RE)BCO Pancake Winding with Metal-as-Insulation," *IEEE Trans. Appl. Supercond.*, vol. 26, no. 3, 2016.

[11] T. Lécrevisse, A. Badel, T. Benkel, X. Chaud, P. Fazilleau, and P. Tixador, "Metal-as-insulation variant of no-insulation HTS winding technique: pancake tests under high background magnetic field and high current at 4.2 K," *Supercond. Sci. Technol.*, vol. 31, no. 5, p. 055008, May 2018.

[12] D. Park, W. Lee, J. Bascunan, H. M. Kim, and Y. Iwasa, "A Cryogen-Free 25-T REBCO Magnet With the Extreme-No-Insulation Winding Technique," *IEEE Trans. Appl. Supercond.*, vol. 32, no. 6, pp. 1–5, Sep. 2022.

[13] W. Lee, D. Park, J. Bascuñán, and Y. Iwasa, "Construction and test result of an all-REBCO conduction-cooled 23.5 T magnet prototype towards a benchtop 1 GHz NMR spectroscopy," *Supercond. Sci. Technol.*, vol. 35, no. 10, p. 105007, Oct. 2022.

[14] F. Dong *et al.*, "On fault-mode phenomenon in no-insulation superconducting magnets: A preventive approach," *Appl. Phys. Lett.*, vol. 121, no. 19, p. 194101, Nov. 2022.

[15] D. Park, J. Bascunan, P. C. Michael, J. Lee, S. Hahn, and Y. Iwasa, "Construction and Test Results of Coils 2 and 3 of a 3-Nested-Coil 800-MHz REBCO Insert for the MIT 1.3-GHz LTS/HTS NMR Magnet," *IEEE Trans. Appl. Supercond.*, vol. 28, no. 3, pp. 1–5, 2017.

[16] Y. Tsui, R. Mahmoud, E. Surrey, and D. Hampshire, "Superconducting and Mechanical Properties of Low-Temperature Solders for Joints," *IEEE Trans. Appl. Supercond.*, vol. 26, no. 3, pp. 1–4, Apr. 2016.

[17] J. Mun, C. Lee, K. Sim, C. Lee, M. Park, and S. Kim, "Electrical Characteristics of Soldered Metal Insulation REBCO Coil," *IEEE Trans. Appl. Supercond.*, vol. 30, no. 4, pp. 1–4, Jun. 2020.

[18] J. Lee, J. Mun, J. Kim, and S. Kim, "Investigation on the Electrical Contact Resistance of Soldered Metal Insulation REBCO Coil," *IEEE Trans. Appl. Supercond.*, vol. 31, no. 5, pp. 1–5, Aug. 2021.

[19] J. Lee, J. Mun, J. Kim, K. Sim, S. Hahn, and S. Kim, "A Study on the Electrical Contact Resistance and Thermal Conductivity of Soldered-Metal Insulation Coil With Conduction Cooling," *IEEE Trans. Appl. Supercond.*, vol. 32, no. 6, pp. 1–5, Sep. 2022.